

# A visual template-matching method for articulation angle measurement

Christopher de Saxe, *Student Member, IEEE*, David Cebon  
Cambridge University Engineering Department  
Cambridge, United Kingdom  
ccd33@cam.ac.uk

**Abstract**—Active control systems for heavy goods vehicles (HGVs) are becoming more sophisticated, necessitating more extensive and sophisticated instrumentation. For articulated HGVs, articulation angle sensing is crucial for most such systems and existing and proposed sensing methods are limited either in terms of commercial feasibility or measurement accuracy. This paper investigates a vision-based system consisting of a single tractor-mounted camera, a template-matching image processing algorithm and an Unscented Kalman Filter. The method is applicable to trailers with planar fronts and requires minimal geometric knowledge of the trailer. A series of tests was performed on a tractor semi-trailer combination. The vision system was able to measure articulation angle with RMS errors of  $0.64^\circ$ – $0.79^\circ$  and maximum errors of  $1.91^\circ$ – $2.76^\circ$ .

**Keywords**—articulation angle; computer vision; template-matching; heavy goods vehicle; semi-trailer; rotation measurement

## I. INTRODUCTION

Active control systems for Heavy Goods Vehicles (HGVs) are becoming more prevalent and sophisticated. This has been partly in response to strict safety-oriented vehicle legislation, and partly in response to trends towards longer and heavier HGVs owing to their established benefits with regard to productivity, efficiency and environmental friendliness [1].

As these systems become more complex, there is a growing need for more complex vehicle instrumentation. In the case of articulated vehicles, there is a common need of these systems for articulation angle sensing. The relevance of articulation angle sensing is highlighted in the path-following steered trailer system in [2], the jackknife prevention system in [3], the autonomous HGV reversing system of [4] and the slip-control braking system proposed in [5]. There is a particular need for systems that are tractor-based. This rules out the conventional sensing technologies adapted for commercial trailer-based articulation sensors (including products from V.S.E, AB Electronic Ltd and Tridec).

## II. RELATED WORK AND MOTIVATION

There has been limited research into establishing a viable means of articulation angle sensing for HGVs. A small number of patents exists to this effect for passenger vehicles with towed trailers [6]–[8]. The use of multiple sensors is proposed including cameras, but the precision of these systems is

unknown and, in cases where cameras are used, details of the image processing methods are not clear.

In work investigating the navigation of small articulated robotic vehicles, Larsson *et al.* [9] used a rotating laser to detect reflective tape of known location affixed to the trailer. The measurements were coupled to an Extended Kalman Filter (EKF). This could yield acceptable accuracy, but is limited in that it requires the existence of known objects on the trailer.

Bouteldja *et al.* [3] developed a jackknife detection system for tractor semi-trailer combinations based solely on the observation of articulation angle. They adopted a state observer and an EKF to estimate the angle and assessed the system through simulation. Although results were not given for the precision of articulation angle measurements, the maximum error in estimated tractor yaw angle was in the region of  $8^\circ$ . A state observer approach was also adopted in the work of Chu *et al.* [10] and Ehlgren *et al.* [11] for tractor semi-trailers. Quantitative errors were not provided in [10], but Ehlgren *et al.* achieved a maximum error of  $5.4^\circ$  in vehicle tests.

In 2009 Schikora *et al.* [12] developed two vision-based systems for the measurement of articulation angle for cars with drawbar trailers and for tractor semi-trailers. Both systems require affixing a predefined pattern to the trailer, and in the latter case an optical encoder ring around the kingpin.

Of particular relevance here is the recent work by Caup *et al.* [13] and by Harris [14]. Caup *et al.* employed a single rear-facing camera to directly measure the articulation angle between a car and a simple drawbar trailer, with assumptions only on the location of the hitch and the maximum length of the drawbar. A simple alpha-beta filter was used to smooth the resultant measurement. In vehicle tests, average errors of  $1.69^\circ$ – $2.19^\circ$  and maximum errors of  $5.48^\circ$ – $7.55^\circ$  were obtained. Harris [14] explored two methods for vision-based articulation angle measurement for heavy goods vehicles with flat-fronted trailers: homography decomposition and stereo vision. A Kalman Filter was employed for smoothing. In CAD-based simulations the homography decomposition method produced maximum errors of  $3.2^\circ$ – $8.4^\circ$ , while vehicle tests with the stereo vision method produced maximum errors of  $3.3^\circ$ – $18^\circ$ . Neither method was refined to the point of real-time capability and so all image sequences were post-processed. Harris proposed a third method, template-matching, which a

preliminary test suggested could be more accurate than the former two methods.

In the light of the above literature, and for feasibility as a control input for HGV control systems, there is a need to explore a system which is tractor-based, requires little or no modifications to the trailer, and which achieves measurement errors less than  $0.5^\circ$ , and ideally in the order of  $0.1^\circ$ . In this work a rear-facing camera setup similar to [12]–[14] is presented, and the template-matching method proposed in [14] is extended, implemented and assessed. For reasonable control action a frame rate of 20 frames per second (fps) is targeted.

### III. TEMPLATE-MATCHING METHOD

The proposed articulation angle measurement system comprises a single, rear-facing camera mounted centrally on the rear of the tractor cabin, viewing the front of the trailer. It is assumed that some degree of visual texture is available on the front face of the trailer, but no constraint on the form or location of this texture is imposed. For development and preliminary testing of the proposed system, a simple 1-degree-of-freedom CAD model of a tractor semi-trailer combination was used as illustrated in Fig. 1.

The system utilises the following procedure:

#### 1) Pre-processing

A single ‘datum’ image of the planar front of the trailer at  $0^\circ$  articulation angle is required initially. For a given trailer with arbitrary visual texture, this can be obtained during simple straight line driving.

With knowledge of simple geometric information about the trailer, and using a planar homography transformation, the datum image can be ‘warped’ through a set of angles in the anticipated articulation range at a chosen increment. (Increment size will limit the achievable precision.) The result is a database of images of the planar face at any angle within the specified range.

#### 2) Online processing

During operation, each image captured by the camera is compared with a subset of warped images from the database (*i.e.* within a defined ‘search range’—see below), yielding a measure of similarity for each database image. The warped image giving rise to the highest similarity with the observed image provides the best estimate of articulation angle.

The current angle estimate provides the midpoint of the database search range for the next frame. A specified search range limits the number of database images to which the observed image will be compared. This has the effect of significantly reducing the number of image comparisons to be computed, but also has the effect of imposing a type of alpha-beta filter. By restricting the anticipated angle change to  $\pm 1^\circ$  per frame, the anticipated articulation rate is capped at  $\pm 1^\circ$  per frame, or  $\pm 20^\circ/s$  for a frame rate of 20 fps.

An Unscented Kalman Filter is used to smooth the measured articulation angles.

Details of the steps are outlined in the following sections.

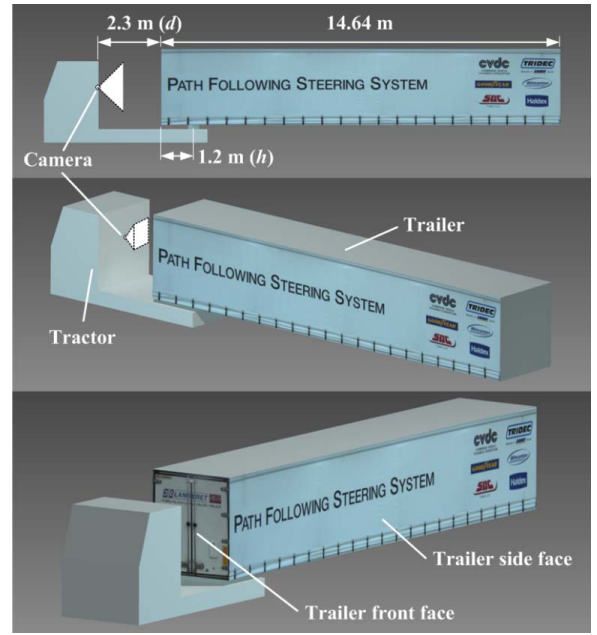


Fig. 1. 1-degree-of-freedom CAD-based model of a tractor semi-trailer combination for preliminary simulation and testing.

#### A. Image Warping

If  $\mathbf{X} = [X, Y, Z]^T$  represents the Cartesian coordinates of a point in 3-D space and  $\mathbf{w} = [u, v]^T$  represents 2-D pixel coordinates in an image, then these may be represented in homogeneous form (denoted by a tilde) as:

$$\tilde{\mathbf{X}} = [\lambda_x X \quad \lambda_x Y \quad \lambda_x Z \quad \lambda_x]^T, \quad \tilde{\mathbf{w}} = [\lambda_w u \quad \lambda_w v \quad \lambda_w]^T \quad (1)$$

where  $\lambda_x$  and  $\lambda_w$  are arbitrary scaling factors.

Assuming an idealised pin-hole camera model with no distortion, the relationship between a point in 3-D space and the image of the point is [15]:

$$\tilde{\mathbf{w}} = \mathbf{K}[\mathbf{R} \mid \mathbf{T}]\tilde{\mathbf{X}}$$

$$= \begin{bmatrix} f \cdot k_u & 0 & u_0 \\ 0 & f \cdot k_v & v_0 \\ 0 & 0 & 1 \end{bmatrix} \begin{bmatrix} r_{11} & r_{12} & r_{13} & T_x \\ r_{21} & r_{22} & r_{23} & T_y \\ r_{31} & r_{32} & r_{33} & T_z \end{bmatrix} \begin{bmatrix} X \\ Y \\ Z \\ 1 \end{bmatrix} \quad (2)$$

Here  $\mathbf{K}$  is the camera calibration matrix and  $\mathbf{R}$  and  $\mathbf{T}$  are the rotation matrix and translation vector describing the transformation from world to camera reference frames.  $\lambda_x$  is arbitrarily set to 1 in the world point but  $\lambda_w$  will in general have non-unit value. The matrix  $\mathbf{K}$  contains information about the intrinsic camera properties, namely the focal length,  $f$ , scaling factors  $k_u$  and  $k_v$ , and the principal point coordinates,  $u_0$  and  $v_0$ . Intrinsic camera parameters are obtained through a suitable camera calibration process such as that of Zhang *et al.* [16].

Consider the case of the camera-trailer system as illustrated in Fig. 2 (a). The camera coordinate system is denoted  $\mathbf{X}_c = [X_c, Y_c, Z_c]^T$ . The parameters  $d$  and  $h$  are assumed known. Considering relative motion between the camera and trailer, a rotation of the trailer of  $\Gamma$  about the hitch point is equivalent to a  $-\Gamma$  rotation of the camera about the hitch point as shown in Fig. 2 (b). If the origin of the world coordinate frame is assumed to be aligned with that of the camera when  $\Gamma = 0^\circ$ , then the motion of the camera is equivalent to  $\mathbf{R}$  and  $\mathbf{T}$  in (2). These may be described in terms of  $\Gamma$ ,  $h$  and  $d$  as follows:

$$\mathbf{R} = \begin{bmatrix} \cos \Gamma & 0 & -\sin \Gamma \\ 0 & 1 & 0 \\ \sin \Gamma & 0 & \cos \Gamma \end{bmatrix}, \quad \mathbf{T} = \begin{bmatrix} (h+d)\sin \Gamma \\ 0 \\ (h+d)(1-\cos \Gamma) \end{bmatrix}. \quad (3)$$

The two views of the planar face are related to each other through a planar homography,  $\mathbf{P}$ . If  $\tilde{\mathbf{w}}_0$  denotes the datum image of the trailer face at  $\Gamma = 0^\circ$ , then the image of the trailer face at a non-zero articulation is

$$\tilde{\mathbf{w}} = \mathbf{P}\tilde{\mathbf{w}}_0. \quad (4)$$

$\mathbf{P}$  is defined as [17]:

$$\mathbf{P}(\Gamma) = \mathbf{K} \left[ s \left( \mathbf{R} + \frac{1}{d} \mathbf{T} \mathbf{N}^T \right) \right] \mathbf{K}^{-1} \quad (5)$$

where  $\mathbf{N}$  is the normal to the observed plane at  $\Gamma = 0^\circ$  (see Fig. 2), and  $s$  is an arbitrary scale factor accounting for the scale ambiguity in the  $(1/d) \cdot \mathbf{T}$  term. In this case,  $\mathbf{N} = [0, 0, 1]^T$ .

Fig. 3 shows the effect of the transformation on the datum image as it is warped through the transformation  $\mathbf{P}$ . By varying  $\Gamma$  through the anticipated articulation range at a specified increment size, the warped image database can be generated.

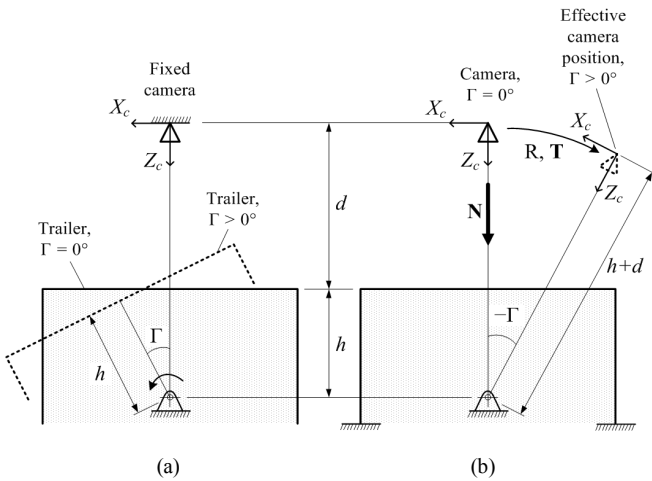


Fig. 2. Top view of the relative motion between trailer and camera. In (a), a camera-fixed reference frame is used, and in (b) a trailer-fixed reference frame is used giving rise to a camera motion model that is better suited to the planar homography mapping.

## B. Image Comparison

With the warped image database generated, estimating the articulation angle is simply a matter of comparing each observed image with a subset of those in the database to find the image with the highest similarity. A number of image similarity metrics exist which are either feature-based or intensity-based. A template-matching measure (intensity-based) was chosen to improve robustness to a potential lack of available feature points. Various developments in the area of template-matching have been proposed (see [18] for an extensive overview). In this case, Lewis' [19] "fast" implementation of two-dimensional normalised cross-correlation was used due to its robustness to brightness and contrast variations (through normalising) and its relative computational efficiency. The basic form of the 2-D normalised cross-correlation function is given by

$$\gamma(u_c, v_c) = \frac{\sum_{x,y} [I(u,v) - \bar{I}_{u,v}] [I_T(u-u_c, v-v_c) - \bar{I}_T]}{\sqrt{\sum_{x,y} [I(u,v) - \bar{I}_{u,v}]^2 \sum_{x,y} [I_T(u-u_c, v-v_c) - \bar{I}_T]^2}} \quad (6)$$

Here  $\gamma(u_c, v_c)$  is the correlation coefficient calculated at each location at which the template,  $I_T$  (in this case the warped image), is overlaid on the search image,  $I$  (in this case the observed image).  $u_c$  and  $v_c$  are horizontal and vertical coordinates over the range of the correlation function.  $\bar{I}_T$  is the mean of the template and  $\bar{I}_{u,v}$  is the mean of the portion of the image overlapped by  $I_T$  at the location  $(u_c, v_c)$ . In Lewis' implementation, calculation of the denominator in (6) is accelerated with the use of pre-computed running sums and, noting that the numerator of (6) is a convolution of two signals, solving the numerator in the frequency domain.

As the template is swept over the search image there will be a peak in the correlation coefficient at the point where the overlaid images best match. An example is shown in Fig. 4 (a) in which the peak is clear near the centre and has a value close to 1. The corresponding overlap of the template with the search image is shown in Fig. 4 (b) (image and template were cropped to reduce computation time). The magnitude of this correlation peak is expected to be highest when the observed image is compared with the warped image nearest to the correct angle.

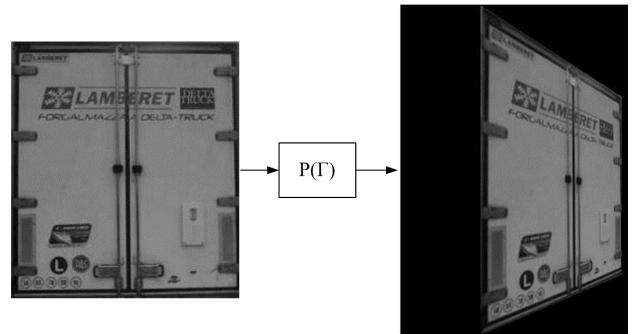


Fig. 3. The effect of the planar transformation,  $\mathbf{P}$ , on the datum image (shown for an arbitrary angle of  $32.7^\circ$ ,  $d$  and  $h$  as in Fig. 1)

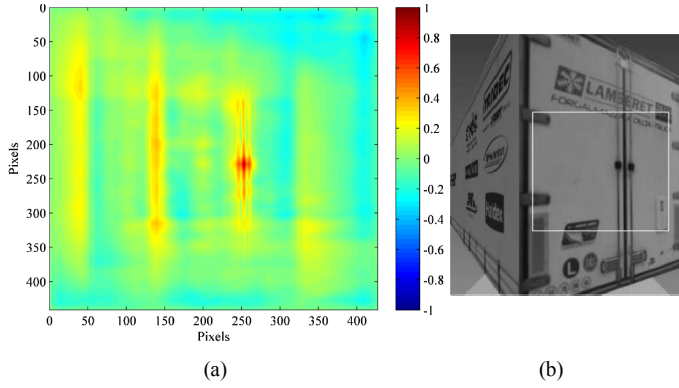


Fig. 4. (a) An example of the cross-correlation function between a warped and observed image taken at  $32.7^\circ$ . In (b) the template has been overlaid on the observed image at the location of the maximum correlation coefficient (very near to 1 in this case), showing the resultant match.

### C. Unscented Kalman Filter

An Unscented Kalman Filter (UKF) [20] was incorporated to smooth the noisy template-matching measurements. For the plant model a 3-degree-of-freedom kinematic ‘bicycle model’ was used as illustrated in Fig. 5. The wheelbase is denoted  $l$ ,  $c$  is the hitch offset,  $\Omega$  is yaw rate, and  $U$  and  $V$  are the longitudinal and lateral velocities at the rear axle respectively. Tractor and trailer parameters are subscripted 1 and 2 respectively. The steer angle is  $\delta$  and the articulation angle is  $\Gamma$ .

By kinematic arguments, we note that:

$$\Omega_1 = (U_1/l_1) \cdot \tan \delta \quad (7)$$

$$\Omega_2 = \Omega_1 + \dot{\Gamma} \quad (8)$$

$$V_2 = (V_1 - c_1\Omega_1) \cdot \cos \Gamma - U_1 \sin \Gamma - \Omega_2 l_2 \quad (9)$$

The kinematic assumption, which is reasonable at low speeds, requires that  $V_1 = V_2 = 0$ . Choosing  $\Gamma$  as the state variable,  $\delta$  as the control input and assuming  $U_1$  to be constant, combining (7)–(9) yields the following non-linear state equation:

$$\dot{\Gamma} = -U_1 \left( \frac{c_1}{l_1 l_2} \tan \delta \cos \Gamma - \frac{1}{l_2} \sin \Gamma - \frac{1}{l_1} \tan \delta \right) \quad (10)$$

In discretised form, (10) is the state transition model. The process noise is assumed to be Gaussian with zero mean and covariance  $Q$ . The measurement model for the filter is simply  $z_k = \Gamma_{T-M}$  where  $\Gamma_{T-M}$  is the raw template-matching measurement output which includes a measurement noise component with covariance,  $W$  (also assumed to be zero mean Gaussian).  $W$  was determined experimentally to be  $(1.45^\circ)^2$  and  $Q$  was set to  $(0.06^\circ)^2$ .

### D. Implementation

A schematic of the overall methodology is given in Fig. 6. A fictitious controller is shown to indicate how the system might be incorporated in a real-time control system. The

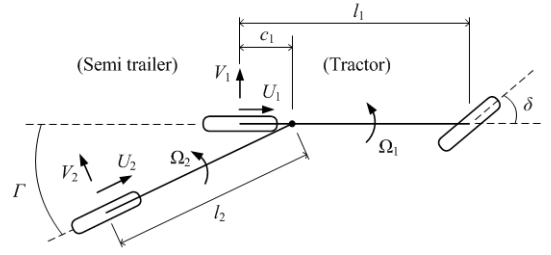


Fig. 5. Kinematic bicycle model for the Unscented Kalman Filter

algorithm was implemented in MATLAB, making use of OpenCV and VLFeat open source libraries [21], [22].

The algorithm assumes that parameters  $d$  and  $h$  are known (see Fig. 2), the observed trailer face is planar, and that the camera is calibrated. In addition, the UKF requires that the wheelbase and axle spacing of both tractor and trailer are known, and that steer angle and speed signals are available.

To reduce computation, observed images were automatically cropped to  $640 \times 200$  while maintaining a suitable view of the trailer front. Warped image size was a maximum of  $640 \times 200$  at  $0^\circ$  (the datum), reducing with increasing warp angle towards the point where face visibility is lost. The increment between database images was set to the target accuracy of  $0.1^\circ$ , and a search range of  $\pm 1^\circ$  was used.

## IV. VEHICLE TESTING

Vehicle testing was carried out on an articulated vehicle combination consisting of a 4x2 Volvo tractor and a tri-axle box-type semi-trailer (with the front axle of the tri-axle group lifted). Although steerable, the trailer axles were not steered during testing. The vehicle is shown in Fig. 7. Parameters  $d$  and  $h$  were measured to be 886 mm and 1575 mm respectively.

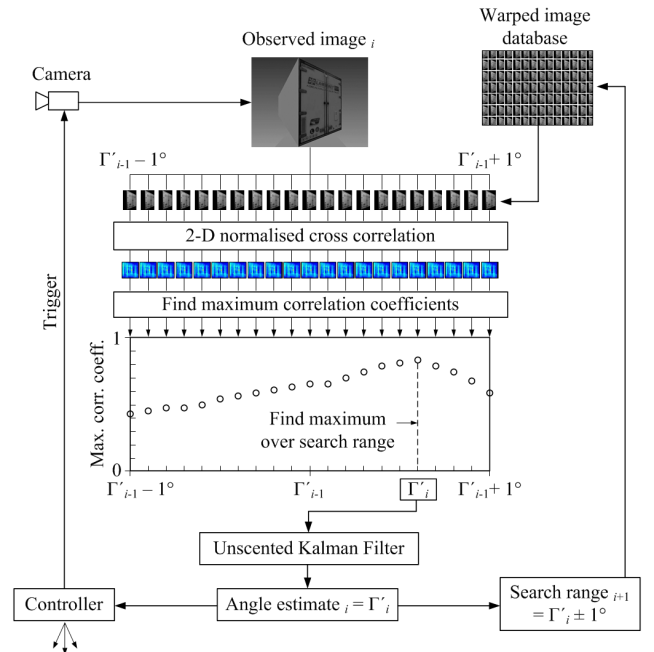


Fig. 6. Flow diagram summarising the template-matching method.

A Point Grey Flea3 USB 3.0 camera with a 2.8 mm wide-angle lens was fitted behind the tractor cabin, capturing 640×480 resolution greyscale images at 20 fps via a dedicated compact computer (see Fig. 7). The vehicle was also fitted with a steering angle sensor, a speed sensor on the tractor drive axle and a trailer-based V.S.E. articulation angle sensor (for reference). Signals from these sensors were logged and synchronised with the camera via a SIMULINK model on a second computer. As the algorithm was not yet real-time capable, image sequences were processed offline after the tests.

Step steer and general driving (arbitrary steer input) manoeuvres were carried out at Bourn airfield near Cambridge. Vehicle speed was approximately constant at 5 km/h and variable in the range 0–10 km/h for step steer and general driving tests respectively. For non-constant speeds,  $U_1$  may be assumed to be constant over a time step (0.05 s). Therefore, although (10) assumes constant velocity, instantaneous values of  $U_1$  were used in the UKF. To account for the effect of tyre scrub of multiple axles, the ‘equivalent wheelbase’ was used in place of  $l_2$  [23].

As the front of the trailer was corrugated, a planar surface was affixed to it along with artificial visual texture (see Fig. 7). Image distortion was corrected using [16]. Lighting conditions were favourable during testing, with no harsh shadows on the trailer face, but brightness levels were variable. A datum image was obtained at the beginning of each test run.

## V. RESULTS

Results for one of the step steer tests are given in Fig. 8 (a). Filtered and unfiltered template-matching measurements (‘T-M’) are plotted against the analogue sensor measurement (the reference). The associated error signals are given in Fig. 8 (c). Results for a general driving test are given in Fig. 8 (b) and (d).

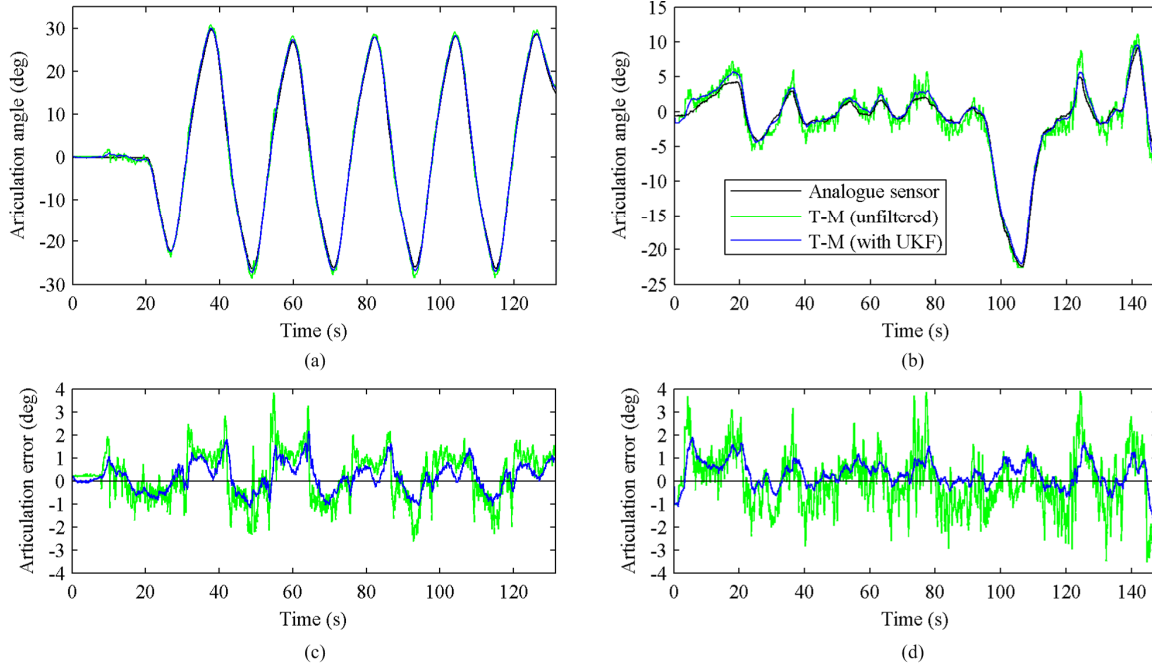


Fig. 8. Vehicle testing results. (a) and (c) show the results and errors for one of three step steer tests, and (b) and (d) show the same for a general driving test. Results are shown with and without the Unscented Kalman Filter.



Fig. 7. The test vehicle, showing the location of the camera and the arbitrary visual texture added to the trailer.

Maximum, RMS and average errors are summarised in Table 1. For the step steer test, results are provided for the test shown in Fig. 8 as well as the average result over three runs.

RMS errors were all less than  $1^\circ$  and near to the target of  $0.5^\circ$ . Maximum errors were in general less than  $3^\circ$ , and these occurred in isolated locations. These large errors could be mostly attributed to undulating sections of the tarmac during which the trailer is seen to pitch and roll (thereby varying the instantaneous values of  $d$  and  $h$ ). Numerical pitch and roll data were not available, and so the sensitivity could not be quantified at this stage. Average errors were relatively consistent and were attributed to a small camera misalignment.

TABLE I. RESULTS SUMMARY

	Step steer		General driving
	Fig. 8(a),(c)	Ave. of 3 tests	Fig. 8(b),(d)
Max. error	2.15°	2.76°	1.91°
RMS error	0.64°	0.79°	0.67°
Ave. error	0.16°	0.21°	0.32°

Average frame rates of just over 1 fps were achieved, significantly off the 20 fps target. However, preliminary tests with down-sampled images have shown that closer to 10 fps may be achievable with a relatively small loss of accuracy.

Given  $d$  and  $h$  of the test vehicle, geometry dictates that the front face of the trailer is no longer visible beyond an angle of 50°, and so it was important that these tests were performed below this limit. The method is extendable to higher angles (and this has been demonstrated in preliminary tests), but this requires a datum image of the side of the trailer which is not obtainable from a simple straight line driving manoeuvre.

## VI. CONCLUSIONS AND FUTURE WORK

A non-contact articulation angle sensor for HGVs utilising a single camera and a template-matching algorithm has been demonstrated. The system assumes limited knowledge of the trailer geometry, a trailer with a planar front, and the existence of some (arbitrary) visual texture on the trailer. Tests with an experimental articulated vehicle illustrated superior accuracy compared to previous work in the published literature. The results showed the system to be sensitive to pitch and roll motion of the trailer, due to an assumed 1-degree-of-freedom motion model. Computational expense was high, with frame rates of approximately 1 fps achieved.

Future work will include the following:

- Methods of significantly improving the frame rate will be explored, including down-sampling and feature-based and histogram methods of image comparison.
- A new multi-degree-of-freedom algorithm will be explored which should be robust to pitch and roll motion and not limited to planar trailer faces.
- Further tests in varying lighting and weather conditions will be conducted. The sensitivity of the algorithm to these conditions will be explored and addressed.

## ACKNOWLEDGMENTS

This work was funded by the Cambridge Commonwealth, European and International Trust (CCEIT), the Council for Scientific and Industrial Research (CSIR, South Africa), and the Cambridge Vehicle Dynamics Consortium (CVDC). At the time of writing the Consortium consisted of the University of Cambridge with the following partners from the heavy vehicle industry: Anthony Best Dynamics, Camcon, Denby Transport, Firestone Industrial Products, Goodyear, Haldex, MIRA, SDC Trailers, SIMPACK, Tinsley Bridge, Tridex, Volvo Trucks, and Wincanton.

## REFERENCES

- [1] OECD/ITF, "Moving freight with better trucks," OECD Publishing, Paris, Apr. 2011.
- [2] R. Roebuck, A. Odhams, K. Tagesson, C. Cheng, and D. Cebon, "Implementation of trailer steering control on a multi-unit vehicle at high speeds," *J. Dyn. Syst. Meas. Control*, vol. 136, no. 2, pp. 1–14 of document 021016, Dec. 2013.
- [3] M. Bouteldja, A. Koita, V. Dolcemasclo, and J. C. Cadiou, "Prediction and detection of jackknifing problems for tractor semi-trailer," in *IEEE Vehicle Power and Propulsion Conference*, 2006, pp. 1–6.
- [4] A. Rimmer, A. Odhams, and D. Cebon, "Autonomous reversing of heavy goods vehicles," in *International Symposium on Heavy Vehicle Transport Technology*, 2012.
- [5] G. Morrison and D. Cebon, "Model-based stabilization of articulated heavy vehicles under simultaneous braking and steering," in *International Symposium on Advanced Vehicle Control*, 2014.
- [6] S. J. Buckley, "Trailer detection system," US 7786849 B22010.
- [7] Y. H. Lee and A. Kade, "Trailer articulation angle estimation," US 8073594 B22011.
- [8] Y. Lu, S. V. Byrne, P. A. VanOphem, and J. D. Harris, "Trailer angle detection system," US 0085472 A12014.
- [9] U. Larsson, C. Zell, K. Hyyppa, and A. Wernersson, "Navigating an articulated vehicle and reversing with a trailer," in *Proceedings of the IEEE International Conference on Robotics and Automation*, 1994, pp. 2398–2404.
- [10] L. Chu, Y. Fang, M. Shang, J. Guo, and F. Zhou, "Estimation of articulation angle for tractor semi-trailer based on state observer," in *International Conference on Measuring Technology and Mechatronics Automation*, 2010, vol. 2, pp. 158–163.
- [11] T. Ehlgren, T. Pajdla, and D. Ammon, "Eliminating blind spots for assisted driving," *IEEE Trans. Intell. Transp. Syst.*, vol. 9, no. 4, pp. 657–665, Dec. 2008.
- [12] J. Schikora, U. Berg, and D. Zöbel, "Berührungslose Winkelbestimmung zwischen Zugfahrzeug und Anhänger," in *Aktuelle Anwendungen in Technik und Wirtschaft*, W. Halang and P. Hollecsek, Eds. Springer Berlin Heidelberg, 2009, pp. 11–20.
- [13] L. Caup, J. Salmen, I. Muharemovic, and S. Houben, "Video-based trailer detection and articulation estimation," in *IEEE Intelligent Vehicles Symposium (IV)*, 2013, pp. 1179–1184.
- [14] M. P. Harris, "Application of computer vision systems to heavy goods vehicles: visual sensing of articulation angle," University of Cambridge, 2013.
- [15] R. Hartley and A. Zisserman, *Multiple View Geometry*, 2nd ed. Cambridge, UK: Cambridge University Press, 2008.
- [16] Z. Zhang, "A flexible new technique for camera calibration," *Pattern Anal. Mach. Intell. IEEE Trans.*, vol. 22, no. 11, pp. 1330–1334, 2000.
- [17] Y. Ma, S. Soatto, J. Košecká, and S. S. Sastry, "Reconstruction from two calibrated views," in *An invitation to 3-D vision: from images to geometric models*, 1st ed., S. S. Antman, J. E. Marsden, L. Sirovich, and S. Wiggins, Eds. New York: Springer Science+Business Media, LLC, 2004, pp. 109–170.
- [18] D. Padfield, "Masked object registration in the Fourier domain," *IEEE Trans. Image Process.*, vol. 21, no. 5, pp. 2706–18, May 2012.
- [19] J. P. Lewis, "Fast normalized cross-correlation," *Vis. Interface*, vol. 10, no. 1, 1995.
- [20] S. J. Julier and J. K. Uhlmann, "Unscented filtering and nonlinear estimation," *Proc. IEEE*, vol. 92, no. 3, pp. 401–422, Mar. 2004.
- [21] G. Bradski, "The OpenCV library," *Dr. Dobb's Journal of Software Tools*. 2000. <http://opencv.org/>
- [22] A. Vedaldi and B. Fulkerson, "VLFeat: An open and portable library of computer vision algorithms." 2008. <http://www.vlfeat.org/>
- [23] C. B. Winkler and J. Aurell, "Analysis and testing of the steady-state turning of multi-axle trucks," in *5th International Symposium on Heavy Vehicle Weights and Dimensions*, 1998, pp. 135–161.